Measured Versus Predicted Performance of Building Integrated Photovoltaics

Mark W. Davis
e-mail: mark.davis@nist.gov

A. Hunter Fanney
e-mail: hunter@nist.gov

Brian P. Dougherty

Heat Transfer and Alternative
Energy Systems Group
National Institute of Standards and Technology
Gaithersburg, MD 20899-8632

The lack of predictive performance tools creates a barrier to the widespread use of building integrated photovoltaic panels. The National Institute of Standards and Technology (NIST) has created a building integrated photovoltaic (BIPV) test bed to capture experimental data that can be used to improve and validate previously developed computer simulation tools. Twelve months of performance data have been collected for building integrated photovoltaic panels using four different cell technologies—crystalline, polycrystalline, silicon film, and triple-junction amorphous. Two panels using each cell technology were present, one without any insulation attached to its rear surface and one with insulation having a nominal thermal resistance value of 3.5 $m^2 \cdot K/W$ attached to its rear surface. The performance data associated with these eight panels, along with meteorological data, were compared to the predictions of a photovoltaic model developed jointly by Maui Solar Software and Sandia National Laboratories (SNL), which is implemented in their IV Curve Tracer software [1]. The evaluation of the predictive performance tools was done in the interest of refining the tools to provide BIPV system designers with a reliable source for economic evaluation and system sizing.
[DOI: 10.1115/1.1532006]

Introduction

Predictive performance tools are an important factor in the success of any technology. An effective performance model would accurately predict the annual energy production given the orientation of the proposed photovoltaic system, typical weather conditions for the geographic region, the nominal performance of the specified BIPV technology, and the proposed coverage area of the BIPV application. The predicted energy production would subsequently be used to compute the energy and cost savings for different cell technologies and system orientations.

The benefits of these predictive tools are obvious. The ability to optimize the performance of BIPV applications allows consumers to maximize the cost effectiveness of the system before installing it. Additionally, the predictive models can demonstrate whether or not a system will be economically feasible.

The accuracy of these tools is key in the overall customer satisfaction. If the predictive models significantly underpredict the amount of BIPV product required for applications, customers may assume that photovoltaics are not as effective as they truly are. Alternatively, predictive models that overpredict the amount of product needed result in poor economic decisions. Predictive tools that either underpredict or overpredict the size of BIPV systems contribute to negative customer satisfaction, which hamper the widespread use of the energy saving technology.

NIST created a building integrated photovoltaic test facility to evaluate BIPV products and predictive tools [2]. The facility includes a *test bed* for side-by-side testing of BIPV products, a solar tracking facility for short-term characterization of BIPV panels, and a rooftop meteorological station. During the calendar year 2000, four different cell technologies, crystalline, polycrystalline, silicon film, and triple-junction amorphous, were present in the *test bed*. Two panels of each cell technology were installed, one panel without backside insulation and one with insulation attached to the rear surface of the panel. The 102-mm (4-in) thick extruded polystyrene insulation has a nominal R-value of 3.5 $m^2 \cdot K/W$ (R-20). Twelve months of performance data was recorded at 5-min intervals, including power output, voltage, current, panel temperature, and meteorological data.

The solar tracking facility is used to characterize the electrical performance of the panels used in the *test bed*. The performance at standard rating conditions, the temperature coefficients, the effect of air mass, and the effect of incident angle are measured for each panel. These parameters are required inputs to the computer simulation tools [3].

The rooftop meteorological station measures the total horizontal, horizontal diffuse, and the direct beam irradiance; the outdoor ambient temperature; and the wind speed and direction. The rooftop data are measured and stored at 5-min intervals throughout the year. Additionally, a small meteorological station is located on the wall at the *test bed*. This station measures the total irradiance in the plane of the panels, the wind speed in the plane of the panels, and the outdoor ambient temperature.

These facilities provide the measurements needed to evaluate BIPV predictive performance tools. The measured *test bed* performance [4] is compared to the performance predicted with the SNL PV model using characterization parameters from the tracking facility and the measured meteorological data. The SNL model is empirical in nature, and it requires many parameters specific to the model. The prediction of the panel's temperature is a key component of any PV model. The temperature of the photovoltaic cells is predicted with IV Curve Tracer using an empirical model. A transient one-dimensional heat transfer model, developed at NIST [5], was substituted for the empirical model. Comparisons were made to predictions using the empirical model and measured data.

Sandia Electrical Performance Model

A number of publications have described the model developed by Sandia National Laboratories to predict the electrical output of photovoltaic panels [6–9]. The equations presented in this paper represent SNL's latest implementation of the model [10]. A premise of this performance model is that the I_{mp}, V_{oc}, and V_{mp} of a photovoltaic module can be described as functions of I_{sc} and the cell temperature. As shown in Eq. (1), the short-circuit current is assumed to be dependant on the beam and diffuse irradiance, air

Contributed by the Solar Energy Division of THE AMERICAN SOCIETY OF MECHANICAL ENGINEERS for publication in the ASME JOURNAL OF SOLAR ENERGY ENGINEERING. Manuscript received by the ASME Solar Energy Division, May 2002; final revision, Aug. 2002. Associate Editor: A. Reddy.

mass, incident angle, and panel temperature. Equations (2)–(6) are used to predict the remaining performance variables (open-circuit voltage, maximum power current, and maximum power voltage) using the short-circuit current. The effective irradiance, E_e, is defined as the ratio of the measured short-circuit current, which is adjusted to the reference temperature, T_o, to the short-circuit current at standard rating conditions. The remaining performance parameters are predicted using the effective irradiance and several empirical coefficients as well as the respective temperature coefficients.

$$I_{sc} = I_{sc_o} \cdot f_1(AM_a) \cdot \left(\frac{(E_b \cdot f_2(AOI) + f_d \cdot E_{diff})}{E_o} \right) \cdot (1 + \overline{\alpha}_{I_{sc}} \cdot (T_c - T_o)) \quad (1)$$

$$E_e = \frac{I_{sc}}{I_{sc_o} \cdot (1 + \overline{\alpha}_{I_{sc}} \cdot (T_c - T_o))} \quad (2)$$

$$I_{mp} = I_{mp_o} \cdot (C_0 \cdot E_e + C_1 \cdot E_e^2) \cdot (1 + \overline{\alpha}_{I_{mp}} \cdot (T_c - T_o)) \quad (3)$$

$$\delta(T_c) = \frac{n \cdot k \cdot (T_c + 273.15)}{q} \quad (4)$$

$$V_{oc} = V_{oc_o} + N_s \cdot \delta(T_c) \cdot \ln(E_e) + \beta_{V_{oc}} \cdot (T_c - T_o) \quad (5)$$

$$V_{mp} = V_{mp_o} + C_2 \cdot N_s \cdot \delta(T_c) \cdot \ln(E_e) + C_3 \cdot N_s \cdot (\delta(T_c) \cdot \ln(E_e))^2 + \beta_{V_{mp}} \cdot (T_c - T_o) \quad (6)$$

$$P_{mp} = V_{mp} \cdot I_{mp} \quad (7)$$

$$f(AM_a) = A0 + A1 \cdot AM_a + A2 \cdot AM_a^2 + A3 \cdot AM_a^3 + A4 \cdot AM_a^4 \quad (8)$$

$$f(AOI) = B0 + B1 \cdot AOI + B2 \cdot AOI^2 + B3 \cdot AOI^3 + B4 \cdot AOI^4 + B5 \cdot AOI^5 \quad (9)$$

A large number of performance parameters that are not provided by manufacturers are required. Temperature coefficients for the maximum power current and voltage, polynomials describing the effect of air mass and incident angles, and an empirical diode factor are a few of the less-common parameters that a system designer would need. However, the developers have provided these obscure values in a large database of parameters for some popular pre-fabricated panels. In the case of custom-fabricated BIPV panels, however, these parameters are not available. Once the parameters are acquired, the implementation of the model is simple, and several programs are available that utilize the SNL model, including IV Curve Tracer [1] and PV-Design Pro [11].

Panel Temperature Prediction Models

The prediction of the panel temperature is an important part of the SNL electrical performance model. The temperature of the panel significantly affects the output voltage and, therefore, the power produced by the panel. The SNL model was run using its own cell temperature prediction method and the NIST cell temperature model. Each model predicts the panel temperature differently. In SNL's model, the temperature on the rear surface of the panel is predicted using the incident irradiance, the ambient temperature, the wind speed, and several empirical coefficients as shown in Eq. (10). Then, using Eq. (11), the temperature at the PV cell, which is the temperature that truly governs the performance of the cell, is predicted using the panel temperature assuming a standard temperature difference between the two. The SNL model developers have provided empirical coefficients [10], Table 1, for three typical panel construction and application scenarios: glass-cell-Tedlar* panel in an open rack, glass-cell-glass panel mounted flat on a roof, and a glass-cell-glass panel in an open rack.

Table 1 SNL thermal model parameters for several panel types and mounting schemes

Panel Type	Mount	a	b	ΔT
Glass/Cell/Glass	Open Rack	−3.473	−0.0595	2
Glass/Cell/Glass	Close Roof Mount	−2.976	−0.0471	3
Glass/Cell/Tedlar	Open Rack	−3.562	−0.0786	3

$$T_m = T_{amb} + E_{POA} \cdot \exp(a + b \cdot WS) \quad (10)$$

$$T_c = T_m + \frac{E_{POA}}{E_o} \Delta T \quad (11)$$

The NIST temperature model [5] uses the approximation of one-dimensional transient heat transfer to predict the temperature of the cell. It uses the beam and diffuse irradiance incident on the panel, the ambient temperature, the effective sky temperature in front and in back of the panel, the wind speed, and the electrical power produced by the panel. The photovoltaic panel is divided into several layers (backside insulation, PV cells, glazing, etc.) according to its construction, and the thickness, density, specific heat, and thermal conductivity are required for each layer. An implicit finite difference scheme is used to determine the temperature throughout the cross-section of the panel, and the cell temperature is calculated as the average of the temperatures in the PV cell layer. The method requires iteration of the temperatures at the two panel surfaces, which makes the NIST PV cell temperature model much more computationally intense than the empirical model used by Sandia National Laboratories.

Modeling Parameters

The SNL's electrical performance model and the NIST cell temperature model require parameters describing the important panel characteristics. Panel manufacturers provide some of these parameters, but each of the models require parameters that are not readily available. The electrical performance model by SNL requires the maximum power, open-circuit, and short-circuit performance ratings, which are normally provided by module manufacturers. The manufacturer's module specifications usually include the short-circuit current and open-circuit voltage temperature coefficients, which are also utilized by SNL's model, but the voltage and current temperature coefficients at the maximum power point that the SNL model requires are not always provided. Manufacturers do not supply the remaining parameters. As mentioned previously, SNL provides a database of empirical coefficients for some common PV panels. Unfortunately, three of the four cell technologies (six of the eight panels) were custom-made for the BIPV *test bed*. Therefore all of the empirical parameters in Eqs. (1)–(7) were measured using the NIST Solar Tracking Facility [3], Table 2.

The thermal models also require a number of parameters. The parameters for the SNL thermal model were discussed previously, Table 1. For the purpose of modeling the NIST BIPV panels, the uninsulated panels will employ the open rack, glass/cell/Tedlar* parameters, and the insulated panels will use the close roof mounted glass/cell/glass parameters. While these parameters do not apply precisely to the mounting of the panels in the NIST BIPV *test bed*, they are the most appropriate of the three options provided by the model developers.

*Certain trade names and company products are mentioned in the text or identified in an illustration in order to adequately specify the experimental procedure and equipment used. In no case does such an identification imply recommendation or endorsement by the National Institute of Standards and Technology, nor does it imply that the products are necessarily the best available for the purpose.

Table 2 Measured electrical performance model parameters for Sandia photovoltaic model

Parameter		Monocrystalline	Polycrystalline	Silicon Film	Triple-Junction Amorphous
Isco	A	4.375	4.250	5.114	4.440
Impo	A	3.961	3.818	4.488	3.613
Voco	V	42.926	41.498	29.614	23.156
Vmpo	V	33.680	32.944	23.165	16.037
α-Isc	A/°C	0.001753	0.002380	0.004683	0.005606
	1/°C	0.000401	0.000560	0.000916	0.001263
α-Imp	A/°C	−0.001543	0.000178	0.001605	0.007348
	1/°C	−0.000390	0.000047	0.000358	0.002034
β-Voc	V/°C	−0.152366	−0.152798	−0.129954	−0.093102
	1/°C	−0.003549	−0.003682	−0.004388	−0.004021
β-Vmp	V/°C	−0.153578	−0.159116	−0.130387	−0.047729
	1/°C	−0.004560	−0.004830	−0.005629	−0.002976
Ns		72	72	56	11
A0		0.935823	0.918093	0.938110	1.100441
A1		0.054289	0.086257	0.062191	−0.061423
A2		−0.008677	−0.024459	−0.015021	−0.004427
A3		0.000527	0.002816	0.001217	0.000632
A4		−0.000011	−0.000126	−0.000034	−0.000019
B0		1.00034	0.99851	0.99898	1.00184
B1		−5.5575E−03	−1.2122E−02	−6.0977E−03	−5.6481E−03
B2		6.5530E−04	1.4398E−03	8.1173E−04	7.2543E−04
B3		−2.7299E−05	−5.5759E−05	−3.3758E−05	−2.9164E−05
B4		4.6405E−07	8.7794E−07	5.6466E−07	4.6957E−07
B5		−2.8061E−09	−4.9190E−09	−3.3714E−09	−2.7387E−09
C0		1.000	1.014	0.961	1.072
C1		0.003	−0.005	0.037	−0.098
C2		−0.538	−0.321	0.232	−1.846
C3		−21.408	−30.201	−9.429	−5.176
n		1.026	1.025	1.357	3.086

Table 3 NIST PV cell temperature model parameters

Layer Parameter	Unit	Monocrystalline	Polycrystalline	Silicon Film	Triple-Junction Amorphous
Glazing		*Glass*	*Glass*	*Glass*	*Tefzel*
Thickness	m	0.006	0.006	0.006	0.000051
Density	kg/m3	2500	2500	2500	1750
Sp. Heat	J/kg K	840	840	840	1050
Th. Cond	W/m K	1.04	1.04	1.04	0.24
Cell		*Silicon*	*Silicon*	*Silicon*	*Silicon*
Thickness	m	0.00086	0.00038	0.00038	0.000001
Density	kg/m3	2330	2330	2330	2330
Sp. Heat	J/kg K	712	712	712	712
Th. Cond	W/m K	148	148	148	148
Backing/Substrate		*Tedlar*/Mylar**	*Tedlar*/Mylar**	*Tedlar*/Mylar**	304*SS*
Thickness	m	0.00017	0.00017	0.00017	0.000125
Density	kg/m3	1475	1475	1475	7900
Sp. Heat	J/kg K	1130	1130	1130	477
Th. Cond	W/m K	0.14	0.14	0.14	14.9
Insulation		*Extruded Polystyrene*	*Extruded Polystyrene*	*Extruded Polystyrene*	*Extruded Polystyrene*
Thickness	m	0.1016	0.1016	0.1016	0.1016
Density	kg/m3	55	55	55	55
Sp. Heat	J/kg K	1210	1210	1210	1210
Th. Cond	W/m K	0.0294	0.0294	0.0294	0.0294

As discussed previously, the NIST PV cell temperature divides the photovoltaic panel into layers according to its construction. The thickness, density, specific heat, and thermal conductivity of each layer are required. The parameters used to model the eight panels are shown in Table 3. The monocrystalline, polycrystalline, and silicon film panels were custom fabricated. Therefore, the materials used in their construction were readily available for thickness measurements. The triple-junction amorphous panel is a pre-fabricated, and the thicknesses of the individual layers were obtained from the manufacturer. The properties for the Tefzel*, Tedlar*/Mylar*, and glass were obtained from specification sheets provided by the respective manufacturers. All of the other property data were obtained from commonly available material property tables.

Model Implementation

In order to compare the measurements made by the BIPV *test bed* with those predicted by the SNL model on an annual basis, the model needed to be applied at 5-min intervals over one year for eight different panels. IV Curve Tracer, which houses the SNL photovoltaic performance model, is used to trace a single I-V curve at specified input conditions. To simplify the use of the BIPV *test bed* meteorological data [4], the SNL model was implemented in a FORTRAN subroutine for use in the TRNSYS [12] frontend. The University of Wisconsin created TRNSYS as an object-oriented application that manages different FORTRAN subroutines. TRNSYS also supplies radiation processors and data reader subroutines for transient applications such as this. The predicted electrical output using the FORTRAN subroutine was compared to the predicted output using IV Curve Tracer. Additionally, a spreadsheet employing the SNL model was obtained from the model developers at Sandia National Laboratories. The spreadsheet had the ability to predict the electrical output of a module over a period of time using meteorological data supplied by the user. The accuracy of the FORTRAN subroutine within TRNSYS as compared to the SNL model was verified by predicting one

Table 4 Monthly SNL and SNL/NIST results for eight panels

	Monocrystalline								Polycrystalline							
	Uninsulated				Insulated				Uninsulated				Insulated			
	SNL		SNL/NIST		SNL		SNL/NIST		SNL		SNL/NIST		SNL		SNL/NIST	
	Diff (%)	R^2	Diff (%)	R^2	Diff (%)	R^2	Diff (%)	R^2	Diff (%)	R^2	Diff (%)	R^2	Diff (%)	R^2	Diff (%)	R^2
January	0.7	0.916	−5.1	0.924	−3.0	0.932	−5.3	0.930	0.6	0.919	−4.4	0.926	−4.8	0.938	−6.5	0.934
February	0.6	0.959	−4.6	0.961	−1.8	0.967	−4.2	0.964	0.2	0.958	−4.5	0.960	−4.1	0.967	−5.9	0.962
March	−1.4	0.971	−5.0	0.969	−3.1	0.972	−4.6	0.967	−1.7	0.969	−5.0	0.967	−5.8	0.969	−6.9	0.963
April	−5.0	0.973	−7.6	0.970	−6.2	0.973	−7.1	0.970	−4.5	0.972	−7.0	0.969	−9.0	0.968	−9.6	0.964
May	−6.3	0.964	−6.9	0.963	−5.9	0.966	−6.4	0.963	−6.8	0.961	−7.3	0.960	−10.4	0.957	−10.7	0.954
June	−5.3	0.962	−5.4	0.961	−4.5	0.964	−4.9	0.961	−6.6	0.957	−6.6	0.957	−10.2	0.952	−10.5	0.950
July	−5.7	0.939	−6.0	0.937	−4.9	0.942	−5.5	0.936	−7.1	0.932	−7.2	0.930	−10.4	0.930	−10.9	0.924
August	−2.8	0.948	−3.4	0.946	−2.3	0.950	−3.2	0.945	−3.6	0.945	−4.0	0.942	−6.8	0.945	−7.5	0.939
September	−1.4	0.940	−3.0	0.937	−1.6	0.942	−2.9	0.935	−2.2	0.937	−3.5	0.934	−5.3	0.939	−6.2	0.931
October	0.4	0.976	−2.5	0.977	0.4	0.980	−2.1	0.978	−0.3	0.976	−2.8	0.976	−2.4	0.981	−4.4	0.977
November	0.8	0.938	−3.8	0.942	−0.7	0.949	−3.1	0.945	1.1	0.943	−3.1	0.946	−2.6	0.958	−4.3	0.952
December	2.8	0.933	−3.9	0.943	−0.8	0.948	−3.5	0.947	3.0	0.939	−3.2	0.948	−2.5	0.958	−4.6	0.955
Total	**−1.1**	**0.947**	**−4.6**	**0.951**	**−2.5**	**0.956**	**−4.2**	**0.953**	**−1.4**	**0.948**	**−4.5**	**0.951**	**−5.4**	**0.958**	**−6.8**	**0.953**

	Silicon Film								Triple-Junction Amorphous							
	Uninsulated				Insulated				Uninsulated				Insulated			
	SNL		SNL/NIST		SNL		SNL/NIST		SNL		SNL/NIST		SNL		SNL/NIST	
	Diff (%)	R^2	Diff (%)	R^2	Diff (%)	R^2	Diff (%)	R^2	Diff (%)	R^2	Diff (%)	R^2	Diff (%)	R^2	Diff (%)	R^2
January	7.9	0.918	0.8	0.935	3.1	0.948	−0.3	0.947	−6.1	0.958	−7.2	0.957	−6.1	0.953	−6.6	0.953
February	6.7	0.954	0.4	0.963	3.1	0.965	−0.5	0.962	−3.8	0.971	−4.7	0.971	−4.3	0.971	−4.8	0.971
March	4.6	0.965	0.1	0.967	1.2	0.969	−1.2	0.963	−3.4	0.973	−4.0	0.973	−4.5	0.973	−4.8	0.972
April	3.6	0.970	0.1	0.969	0.1	0.972	−1.5	0.967	−2.0	0.975	−2.4	0.975	−3.0	0.976	−3.2	0.975
May	4.1	0.956	3.2	0.956	1.5	0.959	0.5	0.956	0.5	0.968	0.4	0.968	0.5	0.968	0.4	0.968
June	6.4	0.947	6.3	0.947	3.8	0.952	2.9	0.950	2.7	0.961	2.7	0.961	2.9	0.962	2.9	0.962
July	4.8	0.923	4.4	0.921	2.4	0.929	1.3	0.922	0.8	0.943	0.7	0.943	1.1	0.943	1.0	0.943
August	6.0	0.937	5.3	0.935	3.8	0.943	2.2	0.936	3.0	0.949	2.8	0.949	3.0	0.950	2.8	0.950
September	4.0	0.930	2.1	0.928	1.8	0.936	−0.2	0.928	−0.7	0.943	−1.1	0.943	−0.9	0.944	−1.1	0.944
October	4.5	0.974	1.0	0.977	3.4	0.979	−0.2	0.977	−0.6	0.984	−1.2	0.984	−1.1	0.983	−1.5	0.983
November	7.5	0.941	1.8	0.950	4.7	0.960	1.2	0.956	0.2	0.967	−0.7	0.968	−1.1	0.968	−1.6	0.968
December	10.0	0.937	2.0	0.955	5.1	0.964	1.2	0.964	1.2	0.970	−0.1	0.972	−0.2	0.968	−0.8	0.968
Total	**6.2**	**0.945**	**1.8**	**0.954**	**3.0**	**0.960**	**0.3**	**0.957**	**−1.0**	**0.967**	**−1.7**	**0.967**	**−1.5**	**0.966**	**−1.9**	**0.966**

day's output of a BIPV *test bed* module using the SNL spreadsheet and the TRNSYS subroutine. The two applications agreed within 0.25% over the day, which indicated successful implementation of the SNL model into FORTRAN.

For the purpose of evaluating the accuracy of these models, the performance and meteorological data recorded during the testing period was divided into blocks of data that were considered suitable for evaluation of performance models. Records that were missing measurements or contained incorrect measurements were not used, and only days with all daylight records present were used in the final analysis. A total of 309 days were analyzed out of a possible 363 days of measured data.

The SNL model and the SNL model outfitted with the NIST PV cell temperature model were applied to the eight panels present in the BIPV *test bed* over the course of a year. The electrical output of the models was compared to the measured electrical output of each panel. At a 95% confidence level, the expanded uncertainty of the measured energy output is $\pm 1.2\%$. Two methods were used to evaluate the quality of the predicted results. Most importantly, the measured accumulated energy was compared to the predicted energy. This quantity is most easily comprehended in terms of a percent difference from the measured value. The second method of comparison was the statistical correlation coefficient, R^2. Unlike the comparison of accumulated energy, the correlation coefficient compares the predicted output at each point. This provides a clearer picture of the precision of the model, but the energy output by the modules is the end goal.

Results

Overall, the performance of the SNL photovoltaic performance model was found to be very good, Table 4. The greatest difference between the predicted and measured accumulated energy using the SNL model was 6.2% in the case of the uninsulated silicon film module. The model agreed with the measured results to within 1.5% for the remaining uninsulated panels. In the case of the insulated panels, the polycrystalline module resulted in the greatest difference (5.4%) between the measured and predicted results. The remaining seven modules agreed within 3% using the SNL model.

Incorporating the NIST temperature model within SNL's photovoltaic model produced mixed results. For the silicon film panel, the predicted energy improved for both the insulated (3.0–0.3%) and uninsulated panel (6.2–1.8%). However, the agreement between the measured and predicted results for the other three insulated panels was not as close as those obtained using the temperature model proposed by SNL.

Looking at the R^2 values, which more accurately indicate the precision of the predictions, the R^2 values for each uninsulated panel improved with the use of the NIST cell temperature model, and the R^2 values decreased for each of insulated panels. For both the insulated and uninsulated cases, the R^2 values of the triple-junction amorphous panels did not change between the two models.

Although the electrical output predictions for the uninsulated panels were closer for the SNL model as opposed to the SNL/NIST model, the NIST temperature model more closely predicted the cell temperature. Figure 1 shows this for the uninsulated monocrystalline panel for two clear days with significantly different outdoor ambient temperatures. The average ambient temperature was 1.5°C on February 5 and 19.5°C on May 4. The expanded uncertainty for both the cell and ambient temperatures is ± 0.3°C at a confidence level of 95%. The average irradiance on February 5 and May 4 was 580 W/m^2 and 210 W/m^2, respectively, which explains the higher panel temperatures seen on the colder day. Similar results for cell temperature prediction were

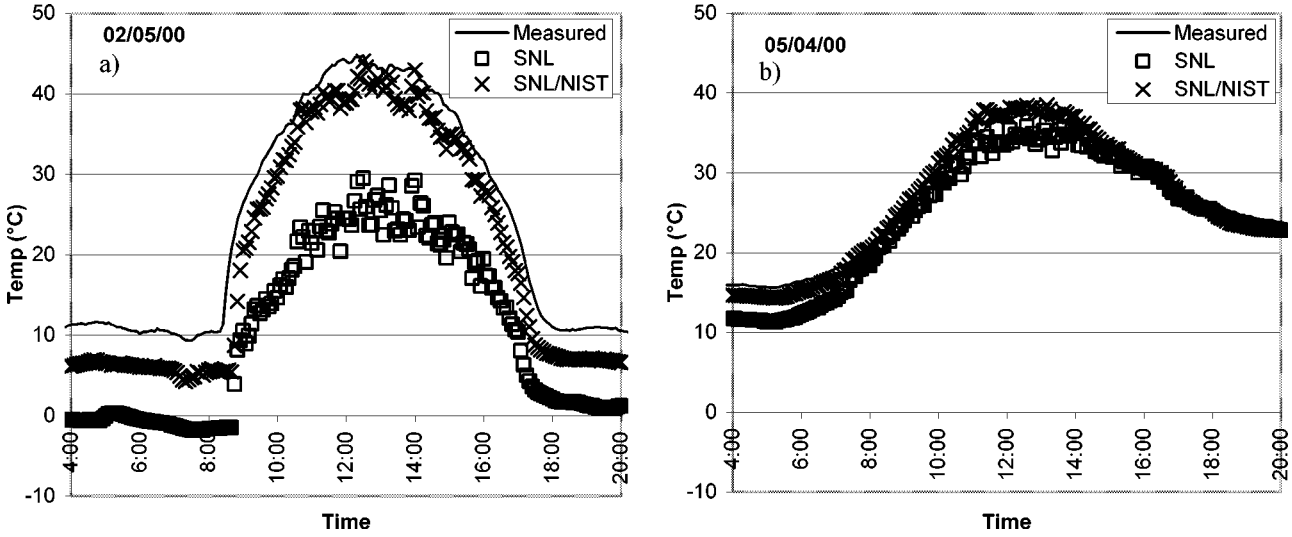

Fig. 1 Measured and predicted cell temperatures for the uninsulated monocrystalline panel for a clear day in *a*) February and *b*) May

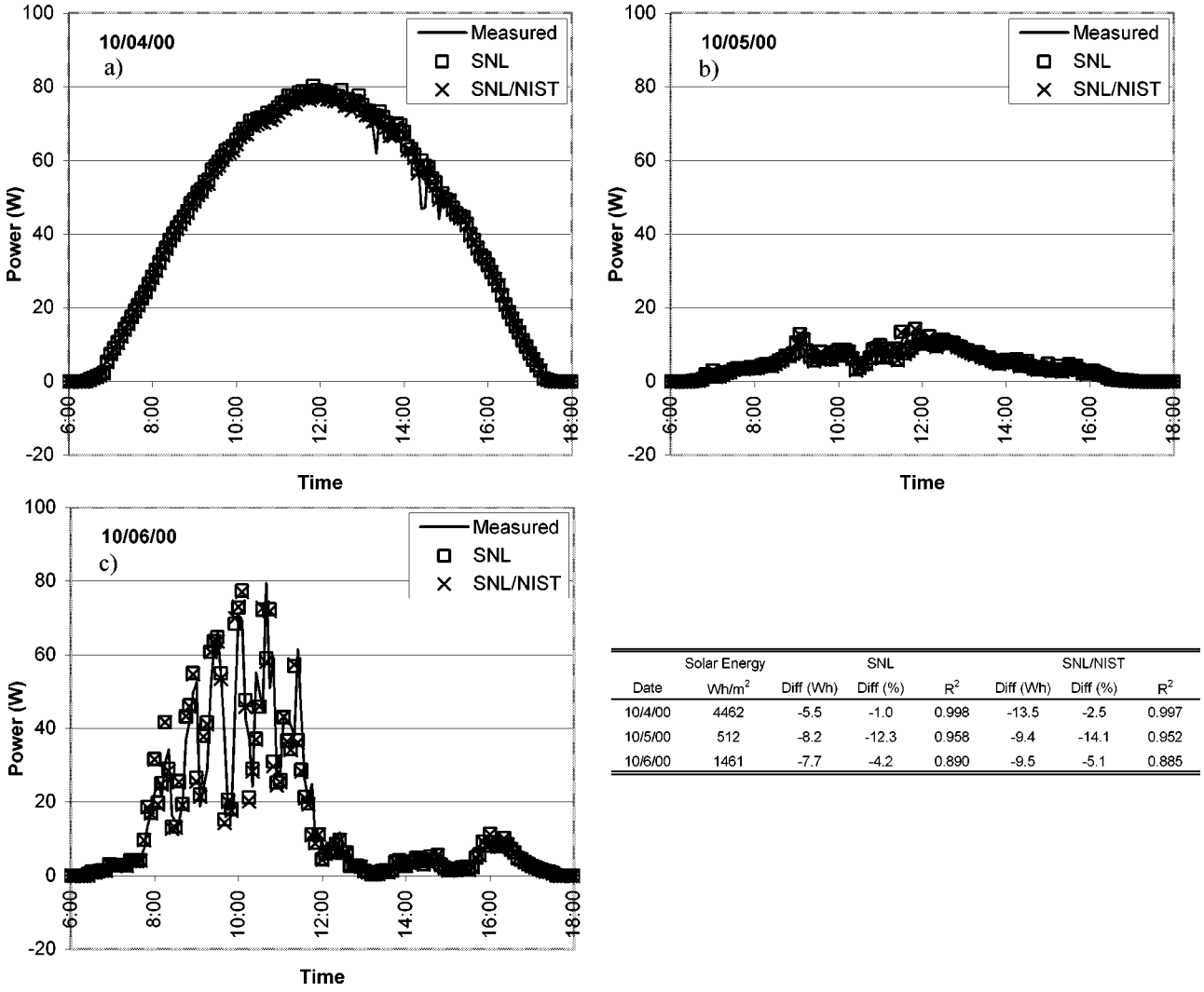

	Solar Energy	SNL			SNL/NIST		
Date	Wh/m^2	Diff (Wh)	Diff (%)	R^2	Diff (Wh)	Diff (%)	R^2
10/4/00	4462	-5.5	-1.0	0.998	-13.5	-2.5	0.997
10/5/00	512	-8.2	-12.3	0.958	-9.4	-14.1	0.952
10/6/00	1461	-7.7	-4.2	0.890	-9.5	-5.1	0.885

Fig. 2 Predicted and measured results for the uninsulated monocrystalline module for *a*) clear, *b*) cloudy, and *c*) partly cloudy days

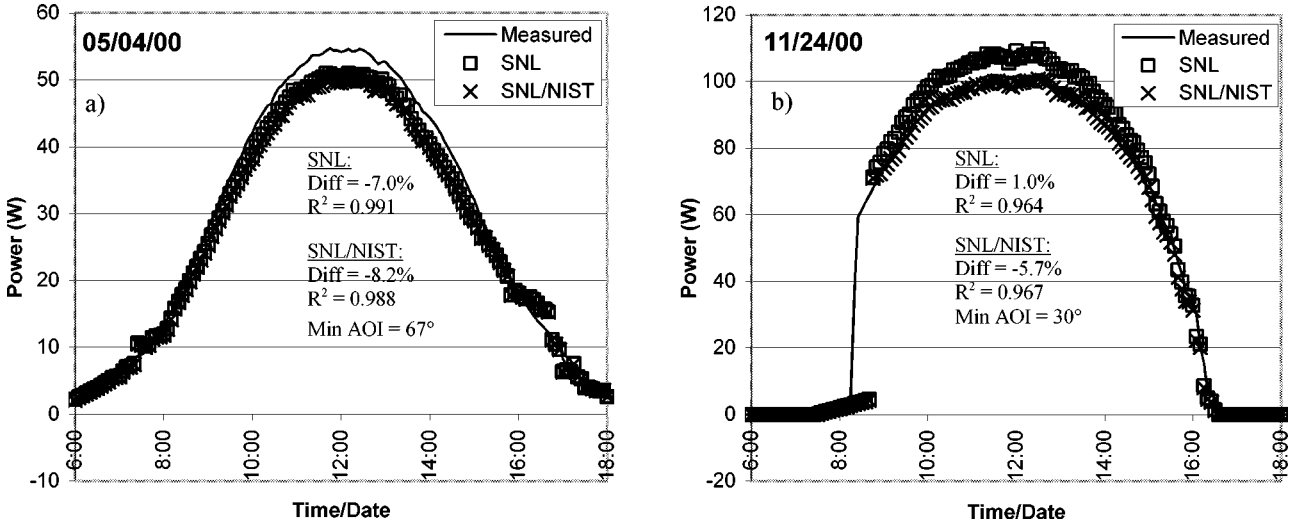

Fig. 3 Measured and predicted power output for a clear day in *a*) May with a high incident angle and *b*) November with a low incident angle

found for all four uninsulated modules. The difference between the models is greater during periods of cold ambient temperatures, Fig. 1. This may be attributed to the fact that the SNL temperature model assumes both sides of the panel are subjected to the outdoor ambient temperature, but in reality, the rear side of the BIPV panels is exposed to controlled indoor conditions. The temperature prediction of both models for the insulated panels closely tracked the measured cell temperatures throughout the year.

It is interesting to note that if the temperature predicted by the SNL model was closer to the measured panel temperature, the SNL electrical performance model would not result in such good agreement. Figure 1 shows that the SNL temperature model underpredicts the uninsulated panel temperatures in the *test bed* during periods of cooler weather. Table 4 shows that the best agreement between the SNL model and the measured results was in those cooler months. In fact, during the warmer months when the NIST and SNL temperature model closely match in their temperature predictions, the differences between the SNL and SNL/NIST models are significantly less. For example, Table 4 shows that for the uninsulated monocrystalline panel, the SNL and SNL/NIST models result in a $+0.6\%$ and -4.6% difference, respectively, in the month of February. However, during the month of June, the differences between the measured results and the two models are almost equal (SNL: -5.3%, SNL/NIST: -5.4%). Except for the triple-junction amorphous panel, which is not as strongly affected by the temperature, similar trends occur for the other panels.

Considering the different methods used to measure the irradiance and power output at each interval, the close agreement between the predicted and measured results is remarkable. The performance model uses the meteorological conditions recorded at 5-min intervals to predict the power output every 5 min. The accumulated energy is assumed to be the product of the power output and the time interval (5 min). The measured electrical energy is also calculated by multiplying the power and the time interval, but the instrument used at the BIPV *test bed* [1] measures the power at 15-s intervals and takes the average over the 5-min period. Thus, on days with quickly changing irradiance values, the predicted and measured values could vary significantly. Additionally, the measurement of the beam irradiance is not directly at the BIPV ''test bed.'' Therefore, on partly cloudy days, the beam irradiance at the *test bed* could be different than the measurement. Figure 2*a*, *b*, and *c* shows measured and predicted power output on three days (clear, cloudy, and partly cloudy) for the uninsulated monocrystalline panel. The percent difference and R^2 values are significantly better for the clear day compared to both the partly cloudy and cloudy days. Although the solar energy was low on the cloudy day, it was relatively steady, which resulted in significantly better R^2 values for the cloudy day than those for the partly cloudy day. The absolute difference between the predicted and measured results for the two models on all three days is shown in the table in Fig. 2. The magnitude of the Watt-hour difference remains approximately the same, but the delivered solar energy varies greatly between the three days. This would seem to indicate that the irradiance level itself does not produce errors in the predictions. The temperature prediction for both models is within 5°C throughout the clear and cloudy days. Due to the quickly changing irradiance, the predicted temperatures on the partly cloudy day were not as close.

The better predictive performance of I-V Curve Tracer on clear days can also be seen in the compiled monthly data. Table 4 shows a dramatic decrease in the R^2 value during the months of July, August, and September for each of the panels. These three months were very cloudy at NIST. Alternatively, October of that year was extremely clear, and it resulted in the highest R^2 value for any month. There were nine clear days in October and only three in the July through September period.

Another reason for poor performance during the summer months may be attributed to the high incident angle throughout the day. Figure 3*a* and *b* shows that the SNL model overpredicts the output power during the winter when the incident angle is relatively low and underpredicts on days when the angle is high. As shown previously, the SNL electrical performance model includes a polynomial function, $f_2(\mathrm{AOI})$, to adjust the transmittance of the glass and absorptance of the PV cells to account for the effect of the incident angle. Additionally, the pyranometer readings are adjusted with respect to the incident angle. The temperatures of the module on these two days are within 6°C at their peak.

Visually, the SNL/NIST model provides an excellent fit for the measured data on November 24, but the percent difference and R^2 values on this day are worse than those for May 4. This discrepancy is due to the early morning shading that occurs in the winter months. A large building lies due East of the BIPV *test bed* and casts a shadow on the test site in the morning. The irradiance measurements are made on the eastern end of the *test bed* below the panels. Therefore, the pyranometers are shaded for a longer period than the modules, especially the monocrystalline modules. Figure 3*b* shows a large underprediction in the early morning that would be expected in this situation.

Conclusion

The photovoltaic model proposed by Sandia National Laboratories was evaluated with respect to the measured electrical output of eight BIPV modules in NIST's BIPV *test bed*. Additionally, the SNL electrical performance model was coupled with the NIST cell temperature model and compared to the measured results. The agreement of both models to the measured data was well within 7% on an annual basis compiling all eight modules. The SNL model resulted in a closer monthly and annual predicted energy output when compared to the SNL model using the NIST cell temperature model. However, it was shown that the NIST cell temperature model more closely predicted the cell temperatures. This discrepancy results from a general underprediction of the power output using the SNL electrical performance model. Additionally, the model performs better on clear days when the irradiance is steady. The model may also underpredict at high incident angles. Overall, annual energy output predictions within 7% of the measured results are quite remarkable.

Nomenclature

- A0–A4 = coefficients for the air mass function, $f_1(AM_a)$
- a,b = empirical coefficients relating the irradiance and windspeed to module temperature
- AM_a = air mass adjusted according to altitude
- AOI = angle between the sun and module (degrees)
- B0–B5 = coefficients for the incident angle function, $f_2(AOI)$
- C_0, C_1 = empirical coefficients relating I_{mp} to the "effective" irradiance
- C_2, C_3 = empirical coefficients relating V_{mp} to the "effective" irradiance
- E_b = beam irradiance (W/m^2)
- E_{diff} = diffuse irradiance (W/m^2)
- E_e = *effective* irradiance
- E_o = reference irradiance, 1000 (W/m^2)
- E_{POA} = irradiance incident on the plane of the module (W/m^2)
- $f_1(AM_a)$ = polynomial describing the spectral influence on I_{sc}
- $f_2(AOI)$ = polynomial describing the effect of incident angle on I_{sc}
- f_d = fraction of diffuse irradiance used by module, 1 for non-concentrating modules
- I_{mp} = current at maximum power point (A)
- I_{mp_o} = maximum power current at $E=1000\ W/m^2$, $T_c=25°C$, $AM_a=1.5$, and $AOI=0$ (A)
- I_{sc} = short-circuit current (A)
- I_{sc_o} = short-circuit current at $E=1000\ W/m^2$, $T_c=25°C$, $AM_a=1.5$, and $AOI=0$ (A)
- k = Boltzmann's constant, 1.380×10^{-23} (J/K·molecule)
- n = empirical diode factor
- N_s = number of cells in series in the module
- P_{mp} = power at maximum power point (V)
- q = elementary charge, 1.60218E-19 (C)
- T_m = temperature on the back surface of a module (°C)
- T_{amb} = ambient temperature (°C)
- T_c = temperature of PV cell
- T_o = reference temperature, 25 (°C)
- V_{mp} = voltage at maximum power point (V)
- V_{mp_o} = maximum power voltage at $E_e=1$ and $T_c=T_o$ (V)
- V_{oc} = open-circuit voltage (V)
- V_{oc_o} = open-circuit voltage at $E_e=1$ and $T_c=T_o$ (V)
- WS = wind speed (m/s)
- $\overline{\alpha}_{I_{mp}}$ = maximum power temperature coefficient normalized with respect to I_{mp_o} (1/°C)
- $\overline{\alpha}_{I_{sc}}$ = short-circuit temperature coefficient normalized with respect to I_{sc_o} (1/°C)
- $\delta(T_c)$ = *thermal voltage* as a function of cell temperature
- $\beta_{V_{mp}}$ = maximum power voltage temperature coefficient (V/°C)
- $\beta_{V_{oc}}$ = open-circuit voltage temperature coefficient (V/°C)
- ΔT = temperature difference between cell and back of module at 1000 W/m^2 (°C)

References

[1] 2000, Sandia Photovoltaic Performance Model I-V Curve Tracer, Maui Solar Energy Software Corp., Haiku, HI.

[2] Fanney, A. H., and Dougherty, B. P., 2001, "Building Integrated Photovoltaic Test Facility," ASME J. Sol. Energy. Eng., **123**(3), pp. 194–199.

[3] Fanney, A. H., Davis, M. W., and Dougherty, B. P., 2002 "Short-Term Characterization of Building Integrated Photovoltaic Panels," *Proc. of Solar 2002: Sunrise on the Reliable Energy Economy*, June, Reno, NV, ASME, New York.

[4] Fanney, A. H., Dougherty, B. P., and Davis, M. W., 2001, "Measured Performance of Building Integrated Photovoltaic Panels," ASME J. Sol. Energy. Eng., **123**(1), pp. 187–193.

[5] Davis, M. W., Fanney, A. H., and Dougherty, B. P., 2000, "Prediction of Building Integrated Photovoltaic Cell Temperatures," ASME J. Sol. Energy Eng., **123**(3), pp. 200–210.

[6] King, D. L., Kratochvil, J. A., and Boyson, W. E., 1997, "Temperature Coefficients for PV Modules and Arrays: Measurement Methods, Difficulties, and Results," *Proc. of 26th IEEE Photovoltaic Specialists Conf.*, Anaheim, CA, pp. 1183–1186.

[7] King, D. L., 1996, "Photovoltaic Module and Array Performance Characterization Methods for all System Operating Conditions," *Proc. NREL/SNL Photovoltaics Program Review*, AIP Press, Lakewood, CO, pp. 347–368.

[8] King, D. L., Kratochvil, J. A., and Boyson, W. E., 1997, "Measuring Solar Spectral and Angle-of-Incidence Effects on Photovoltaic Modules and Solar Irradiance Sensors," *Proc. of 26th IEEE Photovoltaic Specialists Conf.*, Anaheim, CA, pp. 1113–1116.

[9] King, D. L., Kratochvil, J. A., and Boyson, W. E., 1998, "Field Experience with a New Performance Characterization Procedure for Photovoltaic Arrays," *Proc. of 2nd World Conf. and Exhibition on Photovoltaic Solar Energy Conversion*, Vienna, Austria.

[10] King, David L., 2000, "Sandia's PV Module Electrical Performance Model (Version, 2000)," Sandia National Laboratories, Albuquerque, NM.

[11] 2000, PV-Design Pro, Solar Design Studio, v4.0, Maui Solar Energy Software Corp., Haiku, HI.

[12] 2000, TRNSYS, v15, Solar Energy Laboratory, University of Wisconsin, Madison, WI.